Bulgarian Chemical Communications, Volume 50, Special issue H (pp. 181–188) 2018

Study of Fe_3Mo_3N catalyst for ammonia decomposition

S. F. Zaman*, L. A. Jolaloso, A. A. Al-Zahrani, Y. A. Alhamed, S. Podila, H. Driss, M. A. Daous, L. A. Petrov

Chemical and Materials Engineering Department, Faculty of Engineering, King Abdulaziz University, P.O. Box 80204, Jeddah 21589, Saudi Arabia

Received: February 05, 2018; Revised, March 23, 2018

A novel synthesis route, using citric acid as a chelating agent, for the preparation of high surface area γ-Mo_2N and Fe_3Mo_3N bulk samples and their application as catalysts for hydrogen production *via* NH_3 decomposition reaction were investigated. Successful formation of high surface area pure bulk phase of Fe_3Mo_3N (S_{BET} = 24.9 $m^2 g^{-1}$) was confirmed by using XRD, XPS, SEM-EDX, and HRTEM techniques. The Fe_3Mo_3N catalyst showed moderate catalytic activity for ammonia decomposition reaction. It demonstrates 100% conversion of NH_3 at 600 °C at 6000 h^{-1} GHSV. At lower reaction temperatures the Fe_3Mo_3N catalyst has higher catalytic activity than γ-Mo_2N.

Key words: Ammonia decomposition, γ-Mo_2N, Fe_3Mo_3N, Citric acid, Chelating agentл

INTRODUCTION

The high level of environmental pollution and the craving for alternative sustainable clean energy sources is currently a global issue. Hydrogen is a potential alternative fuel due to CO_x-free emissions and its versatility as an energy carrier. Hydrogen has been used as the primary energy source for internal combustion engines or for fuel cells. The problem of using hydrogen as a transportation fuel arises due to the difficulties for finding a proper hydrogen storage system, i.e. as compressed gas or in cryogenic form. Researchers intensively are looking for a suitable hydrogen storage material with high hydrogen density and mild release conditions, which can be safely used in transportation vehicles.

Ammonia, whose synthesis is well matured and in worldwide commercial practice, has been considered as a potential source for the production of hydrogen free of CO_x. NH_3 molecule contains 17.2 wt.% H_2 and agrees with the DOE's criteria to be considered as a commercialisable hydrogen storage material for fuel cell driven transportation vehicles. The cracking of NH_3, an endothermic reaction, must be pursued via a heterogeneous catalytic route. Big number of materials has been tested as catalysts for ammonia decomposition. Unfortunately, ruthenium has been reported to be the most active catalyst [1]. For a short period of time the efforts of the researchers were focused on the ruthenium-based catalysts for ammonia decomposition but considering the cost benefit, the bulk price of ruthenium, which is 50000 times higher than that of iron, thereby calls for the need to develop cheap transition metals-based catalysts with high catalytic performance [2].

Iron is one of the early studied transition metals extensively studied as a catalyst for the decomposition of ammonia reaction for better understanding of ammonia synthesis kinetics over iron based catalysts [3,4]. Very few investigations on iron catalysts for the decomposition of ammonia were reported due to its much smaller activity and stability in contrast to the ruthenium catalysts. This was related to the very strong iron-nitrogen interaction unlike the ruthenium-nitrogen interaction [5]. This strong Fe-N_2 interaction leads to formation subnitrides (stable nitrides) or even bulk nitrides, which were considered in the early studies to be the inhibitors for the ammonia decomposition reaction and eventually deactivating of the catalysts [6–8]. The ammonia decomposition kinetic study reviles that the rate limiting step is the associative desorption of nitrogen over Fe based catalysts [7]. The kinetics follows a Temkin–Pyzhev type rate equation [9].

In this study, we are presenting results of investigation of hydrogen production via ammonia decomposition reaction over high surface area bulk γ-Mo_2N and Fe_3Mo_3N (pure phase) catalysts. Catalysts were prepared using sol-gel method, i.e. using citric acid as a chelating agent. The prepared catalysts were properly characterized using BET, XRD, XPS, SEM-EDX and HRTEM techniques to identify the textural and chemical properties of the prepared catalyst samples.

* To whom all correspondence should be sent
E-mail: zfsharif@gmail.com; sfzaman@kau.edu.sa

EXPERIMENTAL

Used chemicals and methods for catalysts preparation

Ammonium heptamolybdate $(NH_4)_6Mo_7O_{24}.4H_2O$, purity ≥ 99.9%, was received from Fluka Chemical Industry. Iron(II) nitrate hexahydrate $Fe(NO_3)_2.6H_2O$, purity ≥ 99%, was received from Sigma-Aldrich. Citric acid $C_6H_8O_7$, purity ≥ 99%, was received from Techno Pharmchem Industry, Haryana, India. All chemicals were used as obtained.

The sol-gel method using citric acid (CA) as a chelating agent, with molar ratio of CA:Metal = 3, was used to prepare both the γ-Mo_2N and Fe_3Mo_3N catalysts. Fe_3Mo_3N (3.00 g) was prepared by dissolving a desired amount (3.78 g) of ammonium heptamolybdate $(NH_4)_6Mo_7O_{24}.4H_2O$, $Fe(NO_3)_2$ (8.68 g) and citric acid (24.00 g) in 100 cm^3 of deionized water each in separate beakers. Each beaker was placed on a hotplate at 90 °C and stirred uniformly with the help of magnetic stirrer for 30 min. Fe salt solution was then added to the Mo salt solution drop wise and afterwards followed by drop wise addition of CA. The solution mixture was kept on stirring for 4 hours at 90 °C and then the temperature of the hotplate was increased to 150 °C and waited until the solution was turned into a jelly-like substance. The jelly-like solution was then put in a water-bath at 90 °C and aged for 24 hours. After aging, the sample was dried in an oven at 100 °C for 24 hours. The dried sample was pulverized and calcined at 500 °C for 5 hours in stagnant air. The temperature was established by a ramping rate of 5 °C.min^{-1} to form $FeMoO_4$ precursor. Then the precursor underwent nitridation by ammonia to form the Fe_3Mo_3N catalyst.

The nitridation reaction was performed *via* temperature programmed reaction in pure ammonia stream. The process was carried out in a packed bed quartz reactor filled with 1 g of the precursor charged in the reactor at room temperature. Then pure argon was flown at a flow rate of 30 $cm^3.min^{-1}$ through the reactor. The temperature was ramped at 10 °C.min^{-1} until it reached 120 °C. Then the gas was changed to pure ammonia at a flow rate of 400 $cm^3.min^{-1}$ and temperature was increased with a 1 °C.min^{-1} ramping rate till it reached 350 °C. After that the temperature ramping rate was changed to 0.5 °C.min^{-1} and temperature was increased till it reached 700 °C. This temperature was maintained for 2 h keeping the ammonia flow unchanged. Then the gas flow was changed to argon at 700 °C and the reactor temperature was cooled down to room temperature at a ramp rate of 30 °C.min^{-1}. After reaching the room temperature, the mixture of O_2/Ar containing 1.0% O_2 was flown over the catalyst to create a passivated oxidic layer to protect the catalyst from ambient oxygen prior to its exposure to the atmosphere and subjected to catalyst characterization and activity testing experiments.

For the preparation of 2.0 g of γ-Mo_2N catalyst, 3.77 g of ammonium heptamolybdate salt was dissolved in 100 cm^3 deionized water and drop wise addition of CA solution (16.70 g in 100 cm^3 deionized water) in it. Rest of the preparation method follows the similar steps as for Fe_3Mo_3N catalyst.

Characterization Methods

A Nova 2000 Win32 Quantachrome (USA) apparatus was employed to analyze the BET surface area and pore-size distribution of the prepared samples. Each catalyst was degassed at 200 °C for 2 h under vacuum before conducting the measurement.

The Powder X-ray diffraction (XRD) was performed using an Inel Equinox 1000 power diffractometer equipped with a CPS 180 detector (filtered Mo Kα radiation, 40 kV, 30 mA, spinning sample holder). Powder pattern analysis was processed using Match Crystal Impact software (v.1.11e) for phase identification (using both COD and ICSD database), IMAD-INEL XRD software for Rietveld analysis. Data were collected under the same condition for all the samples under investigation. The scanning range was $0 < 2\theta < 120$ with a step size of 0.0284° at an approximate counting time of 1 second per step.

The XPS measurements were carried out in an ultra-high vacuum multi-technique surface analysis system (SPECS GmbH, Germany) operating at a base pressure of 10^{-10} bar range. A standard dual anode X-ray source SPECS XR-50 with Mg-Kα (1253.6 eV) was used to irradiate the sample surface with 13.5 kV, 150 W X-ray power and a take-off-angle for electrons at 90° relative to sample surface plane. The high energy resolution or narrow scan spectra were recorded at room temperature with a 180° hemispherical energy analyzer model PHOIBOS-150 and a set of nine channel electron multipliers MCD-9. The analyzer was operated in Fixed Analyzer Transmission (FAT) and medium area lens modes at pass energy of 20 eV, step size of 0.05 eV and dwell time of 0.3 sec. As the standard practice in XPS studies, the adventitious hydrocarbon C1s line at Binding Energy (BE) of 284.6 eV corresponds to C–C bond has been used as BE reference for charge correction.

TEM analyses of all the catalyst samples were performed using a Tecnai G2 F20 Super Twin device at 200 kV with a LaB6 emitter. The

microscope was fully equipped for analytical work with an energy-dispersive X-ray (EDX) detector having an S-UTW imaging. The scanning transmission electron microscopy (STEM) imaging and all analytical work were performed with a probe size of 1 nm^2 resulting in a beam current of about 0.5 nA. The TEM images and selected- diffraction area (SAD) pattern were collected on an Eagle 2K HR 200 kV CCD camera. The HAADF-STEM EDX and CCD line traces were collected fully automatically using the Tecnai G2 user interface and processed with Tecnai Imaging an Analysis (TIA) software version 1.9.162.

Catalytic activity measurements

Catalytic activity tests were performed at atmospheric pressure in a PID Eng&Tech automated reactor system (Spain) using a fixed bed quartz tube reactor with an external diameter of 6.0 mm. The reactor was charged with 0.10 g of catalyst mixed with 0.1 g of quartz beads to increase the reaction contact area and was held at the center of the heating zone of the reactor furnace. Prior to the reaction, catalysts were activated at 500 °C under nitrogen flow for 1 hour. This was followed by reduction with hydrogen for 5 hours and flushing again with N_2 for 1 hour at the same temperature. After catalyst activation, the reactor temperature was reduced to 300 °C and pure ammonia gas (reactant) was introduced into the reactor at GHSV of 6000 h^{-1}. Then, the temperature was increased stepwise by 50 °C at a ramping rate of 10 °C.min^{-1}. The catalytic test experiments were carried out within the temperature range of 300–600 °C. At each temperature, the reaction was carried out until a steady state regime was established, verified by a relative percentage difference of less than 5% for two successive runs of effluent gas analysis. Effluent gas analysis was performed using an online-connected gas chromatography (GC-450 Varian, USA) equipped with a thermal conductivity detector and a 2.0 m long Porapak Q column.

RESULTS AND DISCUSSION

Catalyst Characterization

The textural properties of the freshly prepared γ-Mo_2N and Fe_3Mo_3N catalysts were studied using N_2-physisorption. The obtained isotherms and the pore size distributions for Fe_3Mo_3N and γ-Mo_2N catalyst are shown in Fig. 1. The BET surface area and the pore volume of γ-Mo_2N were 110.0 $m^2.g^{-1}$ and 0.071 $cm^3\ g^{-1}$. For Fe_3Mo_3N catalyst they were 24.9 $m^2.g^{-1}$ and 0.033 $cm^3.g^{-1}$, correspondingly. Our preparation method has allowed us obtaining Fe_3Mo_3N samples with eight times larger surface area compared to the method used by Srifa *et al.* [10], in which case they have observed BET surface area 8.8 $m^2.g^{-1}$. The increase in surface area is the result of using CA as a chelating agent in the preparation method used by us. CA presence leads to formation of small micelles of metals far apart from each other and thus upon nitridation forming the micro/mesoporous structure.

XRD was used to analyze and identify the phases and crystallinity of the catalysts. Fig. 2 shows the XRD patterns of freshly prepared γ-Mo_2N and Fe_3Mo_3N catalysts (nitridited and passivated). From the analyzed XRD patterns, γ-Mo_2N and MoO_2 phases were registered in the bulk γ-Mo_2N sample. The Mo_2N catalyst had mixed phase of γ-Mo_2N with diffraction peaks (ICSD no. 158843 at 2θ = 43.72, 50.95, 91.00, and 96.27°) and MoO_2 with peaks (ICSD no. 80830 at 2θ = 30.35, 43.31, 63.09, 63.17, 71.29, and 79.36°). The oxidic phase (MoO_2) may arise from the reaction with oxygen present in the atmosphere and also while passivating of the catalysts.

For Fe_3Mo_3N catalyst, only the pure phase of Fe_3Mo_3N (PDF# 01-089-4564) was recorded. No other oxidic or separate Mo or Mo nitride phase was detected as also reported by previous researchers [10,11]. Fig. 2 shows the XRD patterns of fresh and spent γ-Mo_2N and Fe_3Mo_3N catalysts. There are no considerable changes in the structure of Fe_3Mo_3N catalyst except broadening and or increase of the intensity of peaks at some points suggesting that crystallite growth took place in the spent catalyst.

The XPS analysis was done for the freshly prepared nitride catalysts to gain insight view into the oxidation states at the catalyst surface. The XPS spectra for Mo3d region of γ-Mo_2N and Fe_3Mo_3N are shown in Fig. 3a and 3b. The Binding Energies (BE) are tabulated in Table 1. The predominant Mo oxidation states in the γ-Mo_2N catalyst were the Mo^{2+} and/or $Mo^{\delta+}$ which is similar to what was reported by Podila *et al*. [12]. There was also the detection of Mo^{4+} and Mo^{6+} oxidation states in the 3d region. Previous reports [13–15] showed that Mo^{2+} and $Mo^{\delta+}$ oxidation states represent molybdenum nitride. The Mo^{4+} state correspond to MoO_2 while the Mo^{6+} depicts the oxidized form of γ-Mo_2N phase. The piroforic nature of γ-Mo_2N require the sample passivation with 1% O_2/Ar mixture to form a protective layer for the bulk catalyst before it is exposed to the oxygen in the atmosphere for the activity testing and characterization tests, which will inevitably lead to formation MoO_2 phase due to reaction with oxygen.

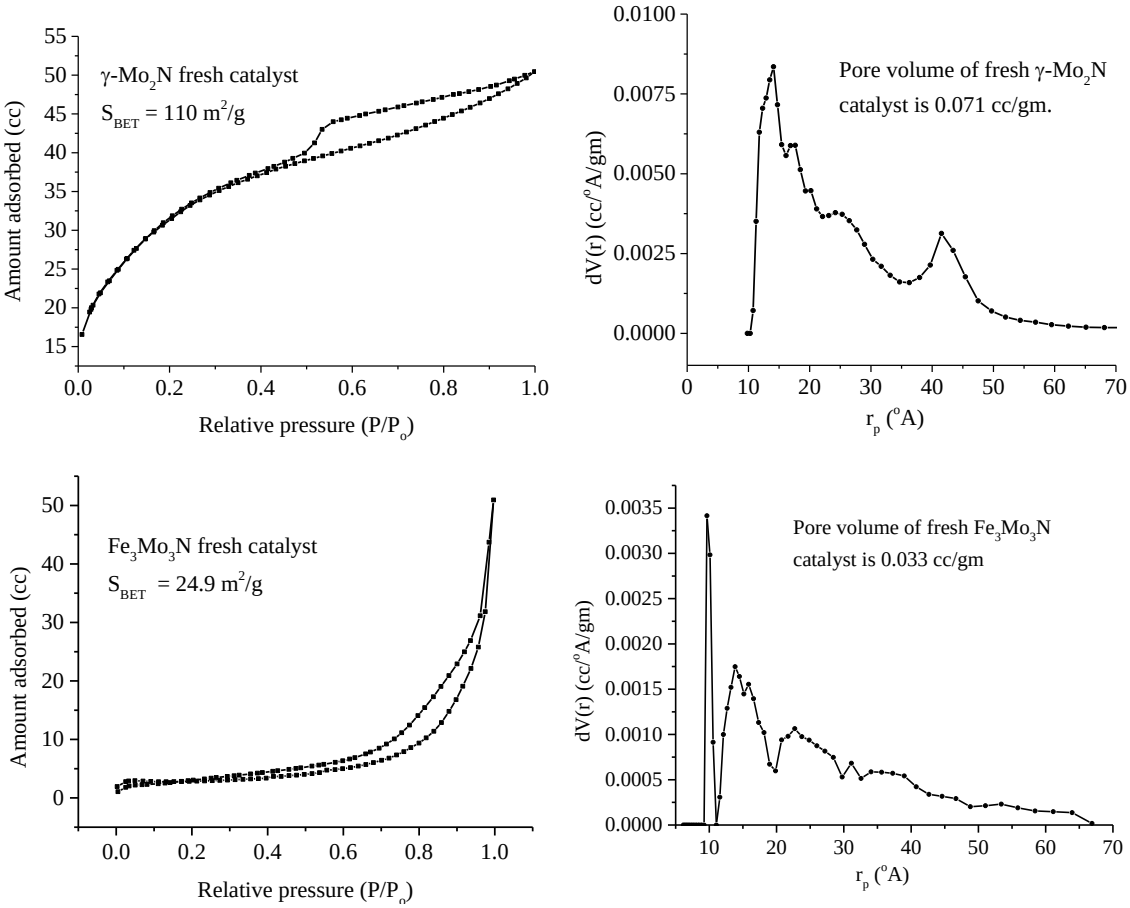

Fig. 1. BET and pore size distribution of γ-Mo_2N and Fe_3Mo_3N catalysts.

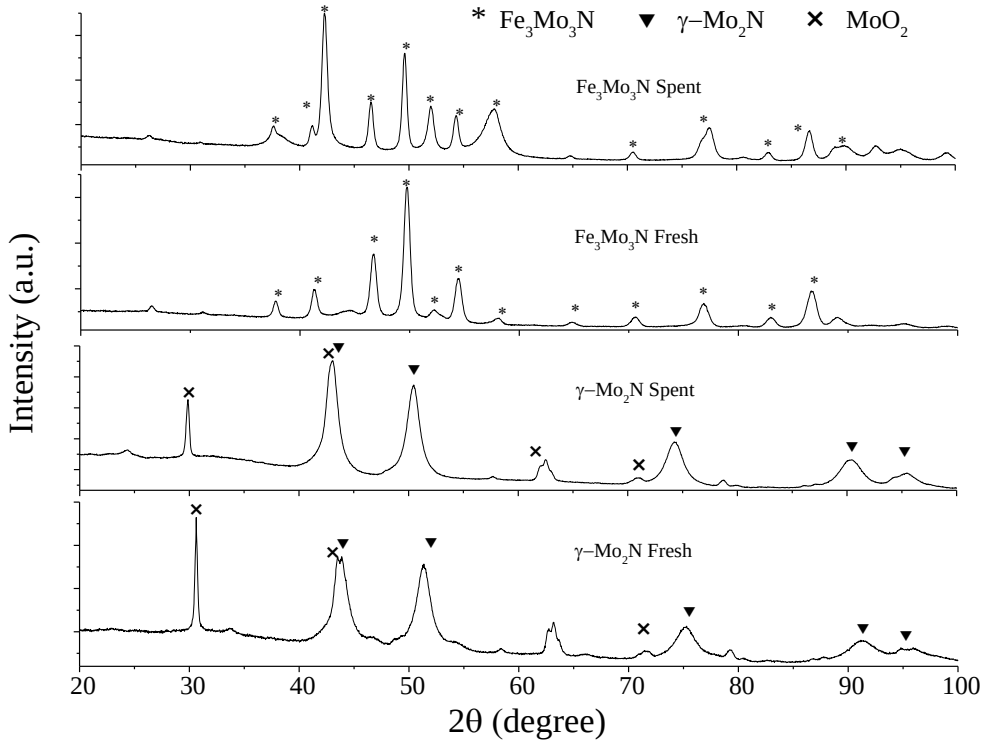

Fig. 2. XRD pattern of fresh and spent Fe_3Mo_3N and fresh Mo_2N catalysts.

For the Mo3d XPS spectra of Fe_3Mo_3N (Fig. 3b) showed typical mixed oxidation state of molybdenum. Higher oxidation states Mo^{5+} and Mo^{6+} are more pronounced compared to γ-Mo_2N sample. The deconvoluted peaks for $Mo3d_{3/2}$ positioned at BE of 227.2, 228.33, and 230.83 eV correspond to Mo^0, $Mo^{+2/\delta}$ and Mo^{+4} oxidation states [16]. According to Perret *et al*. [17] the peak with lower BE of 228.33 eV corresponds to the presence Mo^{+2} ions which represents Fe_3Mo_3N phase and similar conclusion was also drawn by Hada *et al*. [14]. Fig. 3c (values tabulated in Table 1) shows the Fe2p XPS spectral region, which has a notably split spin-orbit components with a range of 15 eV. The BE of 706.8, 708.23, 709.97, and 711.41 eV are assigned for Fe^0, Fe_3O_4 ($Fe^{+2/+3}$), FeO (Fe^{+2}) and Fe_2O_3(Fe^{+3}) oxidation states respectively. The ratio of areas of FeO and Fe_2O_3 oxidation state signals is 1:1, which might have resulted in the formation of highly dispersed Fe_3Mo_3N. The dominant phase occurs at BE of 709.97 eV and is due to possible presence of iron in trivalent state, i.e. Fe_2O_3.

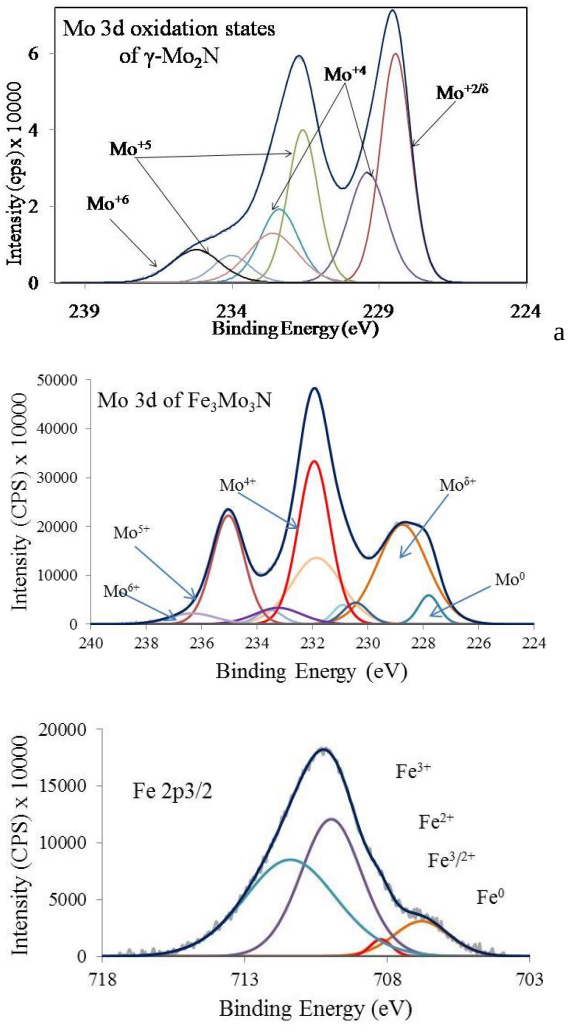

Fig. 3. XPS spectra: a - Mo3d of γ-Mo_2N; b - Mo3d of Fe_3Mo_3N; c - Fe2p of Fe_3Mo_3N.

Table 1. Comparison of the oxidation state of Mo3d with their BE for Fe_3Mo_3N and Mo_2N catalysts.

Oxidation state	Mo BE of catalysts, eV					
	$Fe_{23}Mo_3N$		γ-Mo_2N		$Fe2p_{3/2}$	
	$3d_{3/2}$	$3d_{5/2}$	$3d_{3/2}$	$3d_{5/2}$	Oxidation state	$2p_{3/2}$
Mo^0	230.9	227.8	x	x	x	x
Mo^{2+}	x	x	231.59	228.44	x	x
$Mo^{\delta+}$	231.85	228.75	232.39	229.39	Fe^0	706.8
Mo^{4+}	233.54	230.44	234.01	230.68	Fe^{2+}	709.97
Mo^{5+}	235.04	231.94	x	x	$Fe^{2+/3+}$	708.23
Mo^{6+}	236.34	233.24	235.23	232.61	Fe^{3+}	711.41

SEM-EDS analysis for Fe_3Mo_3N catalyst are shown in Fig. 4. EDX elemental analysis showed that the atomic ratio of Fe:Mo is ~1.17. The results suggest the possible formation of Fe-Mo-N species by the chemical interaction of molybdenum nitride with Fe species.

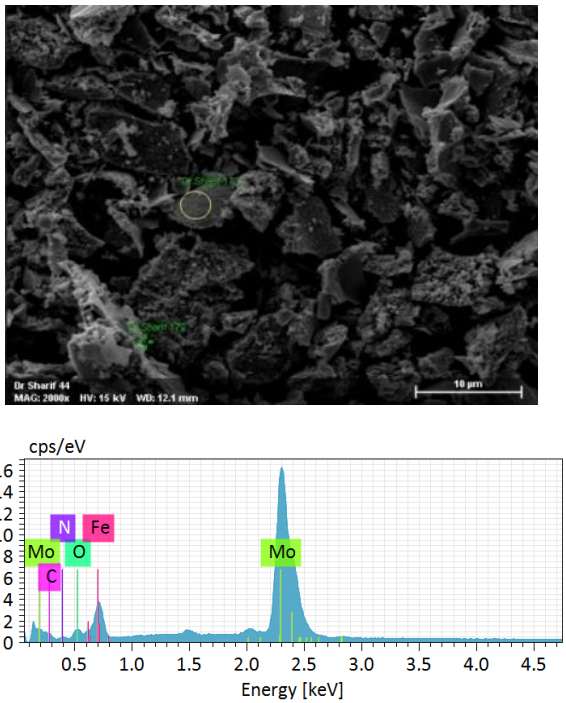

Fig. 4. SEM-EDX analysis of Fe_3Mo_3N catalyst.

HRTEM and selected-area electron diffraction (SAED) pictures of Fe_3Mo_3N are shown in the Fig. 5. The nanodomain of the Fe_3Mo_3N with an average particle size of 5 nm was clearly seen. The selected-area electron diffraction (SAED) pattern of a small representative of Fe_3Mo_3N particle is shown in the bright-field image confirms the existence of (511), (400), (311), and (331) planes, which are belonging to Fe_3Mo_3N. The average particle size of Fe_3Mo_3N measured by HRTEM is 5 nm which is close to the average crystallite size measurement (5.5 nm) using XRD (Mo kα = 0.71 Å) half width data in Scherrer equation.

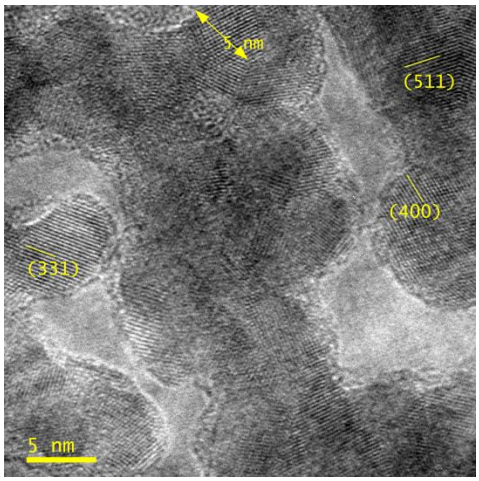

HRTEM image

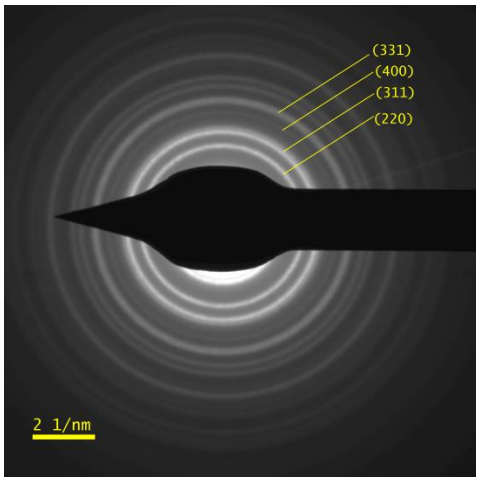

SADE image

Fig. 5. HRTEM and SADE image of Fe_3Mo_3N.

Catalytic activity measurements

The catalytic activity for ammonia decomposition reaction of γ-Mo_2N and Fe_3Mo_3N catalysts was investigated at GHSV of 6000 h^{-1} as a function of temperature at atmospheric pressure. The obtained results are depicted in Fig. 6a. Ammonia decomposition, being an endothermic reaction, showed an increase of ammonia conversion with the increase of temperature. A sharp rise in NH_3 conversion at the beginning of the reaction at 300 °C was observed for Fe_3Mo_3N catalyst, which was not noticed for γ-Mo_2N sample until the reaction temperature reached above 450 °C. At 550 °C the recorded NH_3 conversion over Fe_3Mo_3N, was 78.2%, which is a little better conversion when compared to that reported by Srifa *et al*. [10] at the same temperature and space velocity. On the other hand, at this temperature, γ-Mo_2N catalysts gave only 71.9% conversion. Table 2 shows the experimental data for some previously reported catalysts and the results obtained in this work at 550 °C. The conversion of ammonia at 600 °C on both the Fe_3Mo_3N and γ-Mo_2N catalysts showed approximately equal value with 97.1% and 97.9% NH_3 conversion, respectively. The better results observed in our work might be attributed to the sol-gel preparation method using a chelating agent which gave higher surface area.

Table 2. Activation Energies and NH_3 conversions on different catalysts at 550 °C and GHSV 6000 h^{-1}.

Catalyst	Ammonia conversion, %	Activation energy *Ea*, kJ mol^{-1}	Ref.
Fe_3Mo_3N	78.2	72.9	This work
Fe_3Mo_3N	75.1	88.9	11
γ-Mo_2N	69.2	97.4	11
γ-Mo_2N	71.9	131.3	This work

Experimental results of catalytic activity tests of Fe_3Mo_3N catalyst especially at lower temperatures showed that this catalyst had higher activity compared to γ-Mo_2N catalyst which was an indirect indication that the reaction was actually promoted by the addition of Fe as a catalyst component. Consequently, we can come to the conclusion that adding Fe in the molybdenum nitride structure is the key reason for obtaining the high activity for ammonia decomposition reaction. This effect was connected with lowering the nitrogen association energy over the catalyst induced by the electronic distribution disruption of γ-Mo_2N by the addition of Fe. Also at lower temperatures below 500 °C nitrogen association on the surface is the rate limiting step for the NH_3 decomposition reaction as evidenced by kinetic and DFT investigation of several researchers proposing the following rate equation a for NH_3 decomposition:

$$r_{decomposition} = \frac{P_{NH3}^2}{P_{H2}^3 P_{N2} K_{eq}} r_{synthesis}$$ [18].

Dissociative adsorption of N_2 over Fe based catalyst hindered the ammonia decomposition reaction, whereas Fe modified with Mo and N in the structure enhances the reaction at temperatures about 300 °C suggesting N_2 association is promoted with this structure configuration, i.e. the recombination of N_2 atoms were performed over Fe-Mo-N sites. More experimental evidence is required to confirm the above observation. On the other hand, Srifa *et al*. [10] also reported the decrease in N_2 association energy over $(TM)_xMo_3N$ (TM = Fe, Co, Ni) surfaces compared to Mo_2N surface, which may attribute to the high activity of these bimetallic nitrides compared to γ-Mo_2N for this reaction. This is also in agreement with our observation.

With the increase of temperature higher than 550 °C the inhibition of activity comes from hydrogen

association over the surface (N_2 recombination is no longer a rate limiting step), a well-known phenomenon known as hydrogen poisoning, being the rate limiting step and the two catalysts behave in almost the same way. This is evidenced by kinetic studies conducted by several researchers over different catalysts including Fe based catalysts [7] where ammonia decomposition rate is a function of NH_3 partial pressure of and H_2 only.

The relationship plot of the degree of NH_3 conversion versus temperature for Fe_3Mo_3N and γ-Mo_2N catalysts (Arrhenius plot) is depicted in Fig. 6b. γ-Mo_2N has higher activation energy of 131.29 kJ.mol^{-1} compared to Fe_3Mo_3N, for which the activation barrier drastically reduced to 72.88 kJ.mol^{-1}. This may be the main reason for the high activity of Fe_3Mo_3N. Srifa *et al*. [10] reported. The activation energy of 88.9 kJ.mol^{-1} for Fe_3Mo_3N, which is little higher compared to what we have attained.

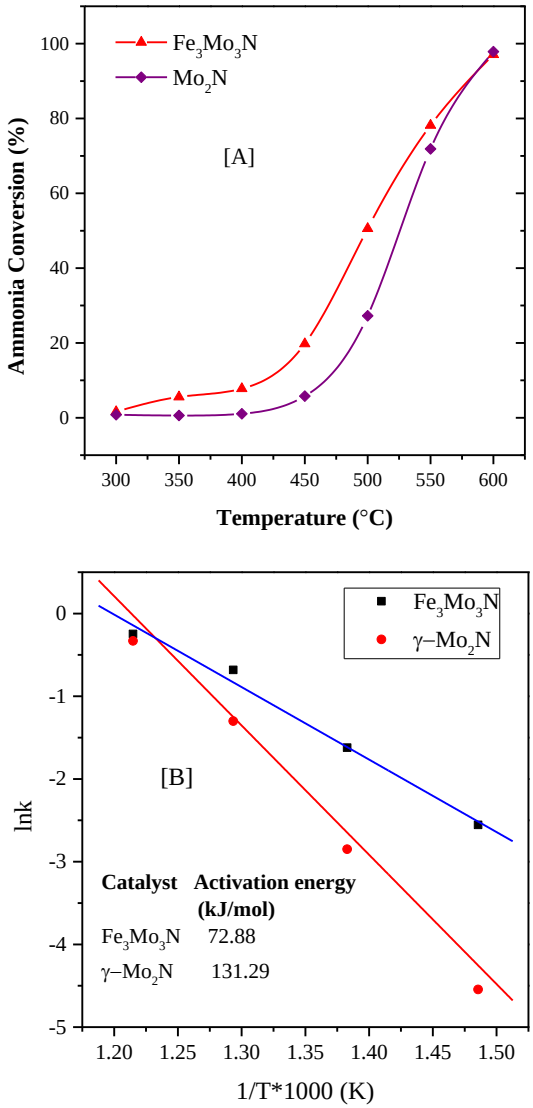

Fig. 6. Catalytic activities (A) and Arrhenius plots (B) of Fe_3Mo_3N and γ-Mo_2N catalysts.

CONCLUSIONS

Ammonia decomposition reaction was investigated using γ-Mo_2N and Fe_3Mo_3N catalysts which were successfully prepared by using sol-gel method and citric acid as a chelating agent. Pure Fe_3Mo_3N phase was successfully obtained from this method of preparation and gave a high surface area of 24.9 m^2g^{-1}. The catalytic activity of this sample was higher compared to catalytic activity of γ-Mo_2N at temperatures below 600 °C.

Acknowledgments: *This project was funded by the Deanship of Scientific Research (DSR) at King Abdulaziz University, Jeddah, under grant no (9-135-36-RG). The authors, therefore, acknowledge with thanks DSR technical and financial support.*

REFERENCES

1. H. Muroyama, C. Saburi, T. Matsui, K. Eguchi, *Appl. Catal. A:Gen.*, **443-444**, 119 (2012)
2. L. Li, Z. H. Zhu, Z. F. Yan, G. Q. Lu, L. Rintoul, *Appl. Catal. A:Gen.*, **320**, 166 (2007).
3. K. S. Love, P. H. Emmett, *J. Am. Chem. Soc.*, **63**, 3297 (1941).
4. S. Dannstadt, Ullmann's Encyclopedia of Industrial Chemistry, Wiley, Weinheim, 2000.
5. R. Schlögl, Ammonia Synthesis, in: Handbook of Heterogeneous Catalysis, G. Ertl, H. Knozinger, F. Schuth, J. Weitkamp, Eds., Wiley-VCH Verlag GmbH & Co. KGaA, 2008
6. A. Mittasch, W. Frankenburg, Early Studies of Multicomponent Catalysts, in: Advances in Catalysis, vol. 2, V. I. Komarewsky, W. G. Frankenburg, E. K. Rideal, Eds., Academic Press, 1950, p. 81–104.
7. T. E. Bell, L. Torrent-Murciano, *Top. Catal.*, **59** 1438 (2016).
8. W. Zheng, Nanomaterials for Ammonia Decomposition, PhD Thesis, Universität Berlin, 2011.
9. W. Arabczyk, J. Zamlynny, *Catal. Lett.*, **60**, 167 (1999).
10. A. Srifa, K. Okura, T. Okanishi, H. Muroyama, T. Matsui, K. Eguchi, C*atal. Sci. Technol.*, **6**, 7495 (2016).
11. J. H. S. Hargreaves, D. McKay, *J. Mol. Catal. A: Chem.*, **350**, 125 (2009).
12. S. Podila, S. F. Zaman**,** H. Driss, Y. A. Alhamed, A. A. Al-Zahrani, M. A. Daous, L. A. Petrov, *Int. J. Hydrogen Energy*, **42,** 8006 (2017)
13. S. Podila, S. F. Zaman, H. Driss, Y. Alhamed, A. A Al-Zahrani, L. A. Petrov, *Catal. Sci. Technol.*, **6,** 1496 (2016)
14. K. Hada, M. Nagai, S. Omi, *J. Phys. Chem. B*, **105,** 4084 (2001).
15. L. A. Jolaoso, S. F. Zaman, S. Podila, H. Driss, A. A. Al-Zahrani, M. A. Daous, L. Petrov, *Int. J. Hydrogen Energy*, DOI: 10.1016/j.ijhydene.2018.01.092, (2018).
16. C. Castillo, G. Buono-core, C. Manzur, N. Yutronic, R. Sierpe, G. Cabello, B. Chornik, *J. Chil. Chem.*

Soc., **61,** 2816 (2016).
17. N. Perret, A. Alexander, S. T. Hunter, P. Chung, J. S. J. Hargreaves, R. F. Howe, M. A. Keane, *Appl. Catal. A: Gen.*, **488,** 128 (2014).
A. Boisen, S. Dahl, J. K. Nørskov, C. H. Christensen, *J. Catal*., **230,** 309 (2005)..

ИЗСЛЕДВАНЕ НА КАТАЛИЗАТОР Fe_3Mo_3N ЗА РАЗЛАГАНЕ НА АМОНЯК

Ш. Ф. Заман*, Л. А. Жолалозо, А. А. Ал-Захрани, Я. А. Алхамед, С. Подила, Х. Идрис, М. А. Даус, Л. Петров

Департамент по химично инженерство и материалознание, Инженерен факултет, Университет „Крал Абдулазис“, п.к. 80204, 21589 Джеда, Саудитска Арабия

Постъпила на 5 февруари 2018 г.; Преработена на 23 март 2018 г.

(Резюме)

Предложен е нов метод за синтез на масивни γ-Mo_2N и Fe_3Mo_3N образци с висока специфична повърхност при използване на хелати. Получените катализатори са изследвани в реакцията на разлагане на амоняк с цел получаване на чист водород без съдържание на CO. Получаването на образец Fe_3Mo_3N (S_{BET} = 24.9 $m^2.g^{-1}$) с висока специфична повърхност е потвърдено чрез използването на XRD, XPS, SEM-EDX, и HRTEM методи. Катализаторът притежава добра активност. При 600 °C и GHSV 6000 h^{-1} конверсията на амоняк достига 100%. При по ниски температури катализатор Fe_3Mo_3N е по- активен от γ-Mo_2N.